JOC Article
pubs.acs.org/joc

Dual Reactivity of Hydroxy- and Methoxy- Substituted *o*-Quinone Methides in Aqueous Solutions: Hydration versus Tautomerization.

Selvanathan Arumugam and Vladimir V. Popik*

Department of Chemistry, University of Georgia, Athens, Georgia 30602, United States

vpopik@chem.uga.edu

Received August 17, 2010

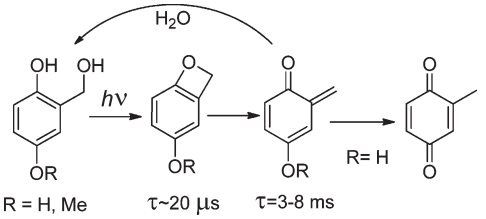

4-Hydroxy-6-methylene-2,4-cyclohexadien-1-one (**1**) and 4-methoxy-6-methylene-2,4-cyclohexadien-1-one (**2**) were generated by efficient ($\Phi = 0.3$) photodehydration of 2-(hydroxymethyl)benzene-1,4-diol (**3a**) and 2-(hydroxymethyl)-4-methoxyphenol (**4a**), respectively. *o*-Quinone methides **1** and **2** can be quantitatively trapped as Diels−Alder adducts with ethyl vinyl ether or intercepted by good nucleophiles, such as azide ion (k_{N3}(**1**) $= 3.15 \times 10^4\ M^{-1}\ s^{-1}$ and k_{N3}(**2**) $= 3.30 \times 10^4\ M^{-1}\ s^{-1}$). In aqueous solution, *o*-quinone methide **2** rapidly adds water to regenerate starting material (τ_{H_2O}(**2**) = 7.8 ms at 25 °C). This reaction is catalyzed by specific acid (k_{H^+}(**2**) $= 8.37 \times 10^3\ s^{-1}\ M^{-1}$) and specific base ($k_{OH^-}$(**2**) $= 1.08 \times 10^4\ s^{-1}\ M^{-1}$) but shows no significant general acid/base catalysis. In sharp contrast, *o*-quinone methide **1** decays (τ_{H_2O}(**1**) = 3.3 ms at 25 °C) via two competing pathways: nucleophilic hydration to form starting material **3a** and tautomerization to produce methyl-*p*-benzoquinone. The disappearance of **1** shows not only specific acid (k_{H^+}(**1**) $= 3.30 \times 10^4\ s^{-1}\ M^{-1}$) and specific base catalysis (k_{OH^-}(**1**) $= 3.51 \times 10^4\ s^{-1}\ M^{-1}$) but pronounced catalysis by general acids and bases as well. The *o*-quinone methides **1** and **2** were also generated by the photolysis of 2-(ethoxymethyl)benzene-1,4-diol (**3b**) and 2-(ethoxymethyl)-4-methoxyphenol (**4b**), as well as from (2,5-dihydroxy-1-phenyl)methyl- (**3c**) and (2-hydroxy-5-methoxy-1-phenyl)methyltrimethylammonium iodides (**4c**). Short-lived ($\tau_{25°C} \approx 20\ \mu s$) precursors of *o*-quinone methides **1** and **2** were detected in the laser flash photolysis of **3a**,**b** and **4a**,**b**. On the basis of their reactivity, benzoxete structures have been assigned to these intermediates.

Introduction

o-Quinone methides (*o*-QMs) are very reactive species that have been implicated as intermediates in many chemical and biological processes.[1−3] The chemical behavior of *o*-QMs resembles that of α,β-unsaturated ketones. However, the zwitterionic resonance form in the former is additionally stabilized by aromatic conjugation, increasing *o*-QMs polarity and enhancing their reactivity.[1,4] *o*-QMs react very rapidly with nucleophiles and undergo efficient Diels−Alder cycloaddition with electron-rich olefins.[1,4] It has been demonstrated that *o*-QMs are efficient dDNA alkylating and cross-linking agents,[1,5] and are believed to be responsible for the cytotoxicity of antitumor antibiotics of mitomycin C and anthracycline families.[6]

(1) Quinone Methides Rokita, S. E., Ed.; ; Wiley Series of Reactive Intermediates in Chemistry and Biology, Vol. 1; Wiley: Hoboken, NJ, 2009.

(2) (a) Wan, P.; Brousmiche, D. W.; Chen, C. Z.; Cole, J.; Lukeman, M.; Xu, M. *Pure Appl. Chem.* **2001**, *73*, 529. (b) Wan, P.; Barker, B.; Diao, L.; Fischer, M.; Shi, Y.; Yang, C. *Can. J. Chem.* **1996**, *74*, 465. (c) Petet, M. G. *Angew. Chem., Int. Ed.* **1982**, *94*, 376. (d) Berson, , J. In *The chemistry of the quinonoid compounds*; Patai, S, Rappoport, Z., Eds.; Wiley: Chichester, UK, 1988; Vol. 2, Part 1, pp 455−536; (e) Van De Water, R. W.; Pettus, T. R. R. *Tetrahedron* **2002**, *58*, 5367. (f) Fischer, M.; Shi, Y.; Zhao, B.-P.; Snieckus, V.; Wan, P. *Can. J. Chem.* **1999**, *77*, 868. (g) Bulger, P. G.; Bagal, S. K.; Marquez, R. *Nat. Prod. Rep.* **2008**, *25*, 254 and references cited therein.

(3) (a) Freccero, M. *Mini Rev. Org. Chem.* **2004**, *1*, 403. *Lignins: Occurrence, Formation, Structure and Reactions*; Sarkanen, K. V., Ludving, C., Eds.; Wiley: New York, 1971. (b) Stowell, J. K.; Widlanski, T. S.; Kutateladze, T. G.; Raines, R. T. *J. Org. Chem.* **1995**, *60*, 6930.

(4) (a) Leo, E. A.; Delgado, J.; Domingo, L. R.; Espinos, A.; Miranda, M. A.; Tormos, R. *J. Org. Chem.* **2003**, *68*, 9643. (b) Chiang, Y.; Kresge, A. J.; Zhu, Y. *J. Am. Chem. Soc.* **2000**, *122*, 9854. (c) Diao, L.; Yang, C.; Wan, P. *J. Am. Chem. Soc.* **1995**, *117*, 5369. (d) Wang, H.; Wang, Y.; Han, K.-L.; Peng, X.-J. *J. Org. Chem.* **2005**, *70*, 4910.

Published on Web 10/06/2010 DOI: 10.1021/jo101613t

o-QMs can be efficiently generated by photodehydration of *o*-hydroxybenzyl alcohol derivatives.[2a,4a−c] The enhanced acidity of phenols in the excited state facilitates intramolecular proton transfer (ESIPT)[7] of the phenolic proton to the oxygen atom in benzylic position.[4a−c] C−O bond heterolysis can be concerted with ESIPT or the loss of water might occur in the ground state after proton transfer is complete.[8] In either case, the formation of *o*-QMs is usually complete within a nanosecond pulse.[4a−c] *o*-QMs also can be generated by photochemical elimination of ammonia or amines from *o*-hydroxybenzylamines.[9]

The major reaction of *o*-QMs in aqueous solutions is rapid addition of water producing *o*-hydroxybenzyl alcohol derivatives. Efficacy enhancement of *o*-QM-based antitumor agents,[1] as well as development of *o*-hydroxybenzyl photolabile protecting groups,[10] requires a better understanding of *o*-QM behavior in this medium. However, only kinetics of hydration of the parent *o*-QM, 6-methylene-2,4-cyclohexadien-1-one, has been investigated in detail.[4b−d] Little is known about the influence of the electronic properties of substituents on the reactivity of oQMs.[4a,5d,11] Our recent studies of *o*-naphthoquinone methides have demonstrated that the presence of an additional electron-rich aromatic ring causes dramatic changes in the mechanism of formation and reactivity of *o*-QM.[11] These results prompted us to investigate the effect of electron-donating substituents on the dynamics of *o*-quinone methide hydration. In the present report we discuss the photochemical generation and reactivity of electron-rich *o*-quinone methides **1** and **2** (Scheme 1).

SCHEME 1

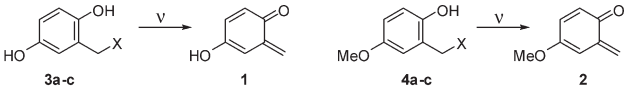

3a-c 1 4a-c 2

X = (a) OH, (b) OEt, (c) $\overset{\oplus}{N}Me_3$

Results and Discussion

o-QMs **1** and **2** are conveniently generated by the photolysis of 2-(hydroxymethyl)benzene-1,4-diol (**3a**) and 2-(hydroxymethyl)-4-methoxyphenol (**4a**); 2-(ethoxymethyl) benzene-1,4-diol (**3b**) and 2-(ethoxymethyl)-4-methoxyphenol (**4b**); as well as from (2,5-dihydroxy-1-phenyl)methyl- (**3c**) and (2-hydroxy-5-methoxy-1-phenyl)methyltrimethylammonium iodides (**4c**).[12] The formation and reactions of *o*-QMs in aqueous solutions were monitored with a nanosecond kinetic spectrometer equipped with pulsed Nd:YAG laser.[12] The product analysis of photochemical reactions of **3a**−**c** and **4a**−**c** was conducted by HPLC, using individual compounds isolated from preparative scale photolyses as references.

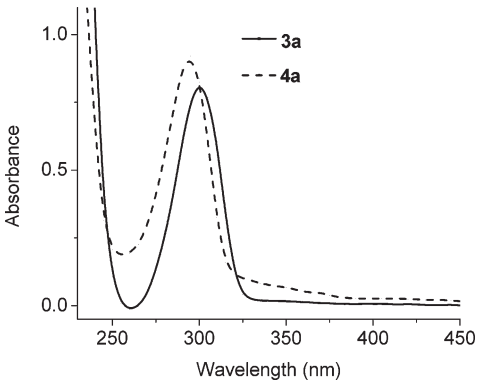

FIGURE 1. UV spectra of ca. 10^{-5} M aqueous solutions of **3a** (solid line) and **4a** (dashed line).

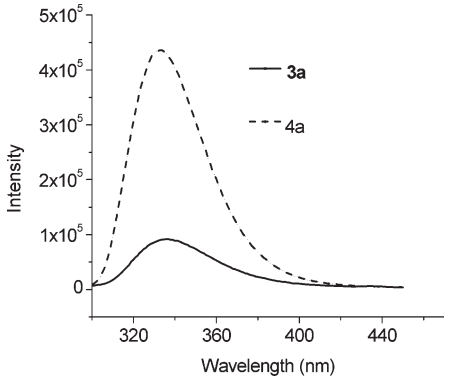

FIGURE 2. Emission spectra at λ_{ex} = 266 nm of ca. 10^{-5} M aqueous solutions of **3a** (dashed line) and **4a** (solid line).

Photophysical Properties and Photochemical Reactivity of *o*-QM Precursors. UV spectra of 2-(hydroxymethyl)benzene-1,4-diol (**3a**) and 2-(hydroxymethyl)-4-methoxyphenol (**4a**) are very similar (Figure 1) and red-shifted by 25−30 nm compared to the spectrum of *o*-hydroxybenzyl alcohol.[13] A major absorption band of **3a** lies at 295 nm (log ε = 3.91) and of **4a** at 300 nm (log ε = 3.97). Both *o*-QM precursors are fluorescent showing emission band with λ_{max} at 333 (**3a**) and 336 nm (**4a**) (Figure 2). The quantum yield of fluorescence is higher for 2-(hydroxymethyl)-4-methoxyphenol (**4a**, Φ_{Fl} = 0.16 ± 0.01) than for **3a** (Φ_{Fl} = 0.050 ± 0.002).[12,14] This emission hinders monitoring of laser flash-induced transformation of **3a** and **4a** at shorter wavelengths, but the intensity of fluorescence dies off above 400 nm and thereby allows us

(5) (a) Wang, P.; Song, Y.; Zhang, L. X.; He, H. P.; Zhou, X. *Curr. Med. Chem.* **2005**, *12*, 2893. (b) Freccero, M.; Di Valentin, C.; Sarzi-Amade, M. *J. Am. Chem. Soc.* **2003**, *125*, 3544. (c) Weng, X.; Ren, L.; Weng, L.; Huang, J.; Zhu, S.; Zhou, X.; Weng, L. *Angew. Chem., Int. Ed.* **2007**, *46*, 8020. (d) Weinert, E. E.; Dondi, R.; Colloredo-Melz, S.; Frankenfield, K. N.; Mitchell, C. H.; Freccero, M.; Rokita, S. E. *J. Am. Chem. Soc.* **2006**, *128*, 11940. (e) Wang, P.; Liu, R.; Wu, X.; Ma, H.; Cao, X.; Zhou, P.; Zhang, J.; Weng, X.; Zhang, X.-L.; Qi, J.; Zhou, X.; Weng, L. *J. Am. Chem. Soc.* **2003**, *125*, 1116. (f) Richter, S. N.; Maggi, S.; Mels, S. C.; Palumbo, M.; Freccero, M. *J. Am. Chem. Soc.* **2004**, *126*, 13973. (g) Colloredo-Mels, S.; Doria, F.; Verga, D.; Freccero, M. *J. Org. Chem.* **2006**, *71*, 3889.

(6) (a) Han, I.; Russell, D. J.; Kohn, H. *J. Org. Chem.* **1992**, *57*, 1799. Li, V.-S.; Kohn, H. *J. Am. Chem. Soc.* **1991**, *113*, 275. (b) Tomasz, M.; Das, A.; Tang, K. S.; Ford, M. G. J.; Minnock, A.; Musser, S.; Waring, M. J. *J. Am. Chem. Soc.* **1998**, *120*, 11581. (c) Egholm, M.; Koch, T. H. *J. Am. Chem. Soc.* **1989**, *111*, 8291. (d) Gaudiano, G.; Frigerio, M.; Bravo, P.; Koch, T. H. *J. Am. Chem. Soc.* **1990**, *112*, 6704.

(7) (a) Lahiri, S. C. *J. Sci. Ind. Res.* **1979**, *38*, 492. Van der Donckt, E. *Prog. React. Kinet.* **1970**, *5*, 273. (b) Ireland, J. F.; Wyatt, P. A. H. *Adv. Phys. Org. Chem.* **1976**, *12*, 131. (c) Shizuka, H.; Tobita, S. *Mol. Supramol. Photochem.* **2006**, *14*, 37. (d) Tolbert, L. M.; Solntsev, K. M. *Acc. Chem. Res.* **2002**, *35*, 19.

(8) (a) Wan, P.; Barker, B.; Diao, L.; Fischer, M.; Shi, Y.; Yang, C. *Can. J. Chem.* **1995**, *74*, 465. (b) Yijian, S.; Wan, P. *Can. J. Chem.* **2005**, *83*, 1306.

(9) Nakatani, K.; Higashida, N.; Saito, I. *Tetrahedron Lett.* **1997**, *38*, 5005.

(10) (a) Kostikov, A.; Popik, V. V. *Org. Lett.* **2008**, *10*, 5277. (b) Kostikov, A.; Popik, V. V. *J. Org. Chem.* **2007**, *72*, 9190.

(11) Arumugam, S.; Popik., V. V. *J. Am. Chem. Soc.* **2009**, *131*, 11892.

(12) See the Supporting Information.

(13) Kammerer, B.; Kahlich, R.; Biegert, C.; Gleiter, C. H.; Heide, L. *Phytochem. Anal.* **2005**, *16*, 470–478.

(14) (a) Wang, Y.-H.; Zhang, H.-M.; Liu, L.; Liang, Z.-H.; Guo, O.-X.; Tung, C.-H.; Inoue, Y.; Liu, Y.-C. *J. Org. Chem.* **2002**, *67*, 2429. (b) Berlman, I. B. *Handbook of Fluorescence Spectra of Aromatic Molecules*; Academic Press: New York, 1971; p 473.

to monitor the formation and the decay of *o*-QMs **1** and **2** at wavelengths > 400 nm.

Prolonged irradiation of an aqueous solution of *o*-QM precursor **3a** (pH 6.96 ± 0.06) with 300 nm light yielded methyl-*p*-benzoquinone **5** as the only photoproduct. The quantum yield of the formation of **5** is $\Phi_{3a} = 0.060 \pm 0.005$. Since competing hydration of the *o*-QM **1** regenerates the starting material **3a** and thus is undetectable, we have explored the aqueous photochemistry of the corresponding ethyl ether **3b**. Low conversion (~15%) photolysis of **3b** in aqueous biphosphate buffer solutions at pH 6.96 ± 0.06 yielded diol **3a** as the major product (76(±2)%) and 2-methyl-1,4-benzoquinone (**5**) as the minor product (19(±2)%) with quantum efficiency $\Phi_{3b} = 0.31 \pm 0.01$ (Scheme 2, Table 1).

SCHEME 2

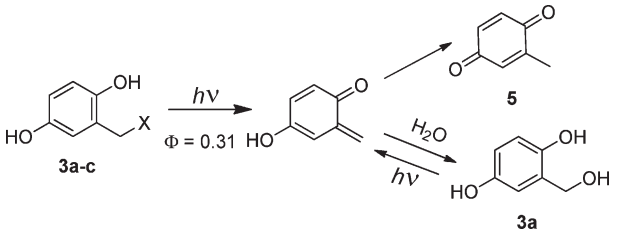

TABLE 1. Photolysis of *o*-QM precursors 3a−c and 4b,c in Aqueous Biphosphate Buffer Solutions (pH 6.96 ± 0.6)

o-QM precursor	yield of **3a** or **4a**/% (conversion)[a,b]	yield of **5**/% (conversion)[a,b]	yield of **6** or **7**/% (conversion)[a,c,d]
3a	N/A	96 ± 2 (10%)	94 ± 1 (93%)
3b	76 ± 2 (15%)	19 ± 2 (15%)	93 ± 1 (99%)
	31 ± 2 (81%)	59 ± 2 (81%)	
3c	72 ± 1 (12%)	22 ± 2 (15%)	95 ± 1 (98%)
	37 ± 3 (75%)	57 ± 2 (81%)	
4b	94 ± 3 (16%)	−[e]	92 ± 2 (98%)
	73 ± 3 (80%)		
4c	96 ± 2 (15%)	−[e]	96 ± 1 (99%)
	76 ± 3 (82%)		

[a] $\lambda_{irr} = 300$ nm. [b] Ca. 3×10^{-4} M in water. [c] Ca. 3×10^{-4} M solutions of the substrate; ca. 0.03 M ethyl vinyl ether. [d] In 50% CH_3CN_{aq}. [e] Not detected.

At higher conversion, the chemical yield of **5** increases as the primary product, diol **3a**, is also photoactive. The chemical yields of the products upon 300 nm irradiation of **3b** are near quantitative (~90%) even at higher conversion (> 80%) as the benzoquinone product **5** does not have significant absorption at the irradiation wavelength (Table 1).

Photolysis of aqueous solutions of *o*-QM precursor **4a** with 300 nm light did not produce any detectable amounts of new products due to the rapid and efficient rehydration of QM **2** to yield back the starting material. On the other hand, irradiation of the aqueous solution of ethyl ether **4b** resulted in a rapid consumption of the substrates and the formation of **4a** (Scheme 3).

The quantum yield for the photoelimination of ethanol from **4b** at 300 nm is $\Phi_{4b} = 0.28 \pm 0.01$.[12] The chemical yield of **4a** produced in this reaction is almost quantitative at low conversions, but is somewhat reduced at longer irradiation times, apparently due to secondary photochemical processes (Table 1). However, no new photoproducts were detected by HPLC or isolated by flash chromatography, even after prolonged irradiation of **4a**.

SCHEME 3

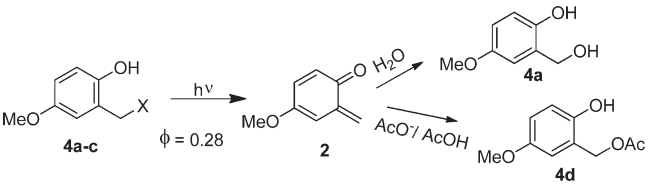

This observation suggests that the secondary photoproducts are most likely *o*-QM oligomers, which are trapped on the column.[15]

o-Hydroxybenzyltrimethylammonium salts are also known to generate *o*-QMs upon irradiation.[16] To compare the reactivity of *o*-QM generated from an alternative source, we have studied the photochemistry of (2,5-dihydroxybenzyl)trimethylammonium iodide (**3c**) and (2-hydroxy-5-methoxybenzyl)trimethylammonium iodide (**4c**). 300 nm irradiation of the ammonium salt **4c** in aqueous solution cleanly produces the diol **4a**. As in the case of ethyl ether **4b**, low conversion photolysis of **4c** gave a quantitative yield of the product, while at high conversion the yield dropped to 76% without formation of detectable byproduct (Table 1). Irradiation of **3c** in aqueous biphosphate buffer solutions at pH 7.0 yielded both diol **3a** and *p*-quinone **5**. The ratio of hydration to ketonization products was similar to that obtained in the photolysis of the ether **3b** (Table 1). This observation provides additional support for the mechanism of formation of **3a** and **5** from *o*-QM **1**.

It is interesting to note that the ratio of hydration to ketonization products (**3a**/**5**) depends on the acidity of the solution. Thus, diol **3a** is the major product of the photolysis of **3b** at neutral pH (Table 1) and in aqueous perchloric acid at or below 10^{-3} M concentration (Table 2). At higher acidities, ketonization to produce *p*-quinone **5** becomes the predominant pathway of *o*-QM **1** decay. *o*-QM **2** in aqueous solutions produces only diol **4a** irrespective of the media acidity. No new products were detected in the photolyses of **3b** and **4b** in perchloric acid solutions.

TABLE 2. Photolysis of 3b and 4b in Aqueous Perchloric Acid Solutions

o-QM precursor	$[HClO_4]$/M	yield of **3a** or **4a**/% (conversion)	yield of **5**/% (conversion)
3b	0.001	64 ± 2 (20%)	34 ± 2 (20%)
3b	0.01	34 ± 2 (20%)	63 ± 2 (20%)
3b	0.05	23 ± 2 (22%)	75 ± 2 (22%)
3b	0.1	15 ± 1 (21%)	80 ± 2 (21%)
4b	0.001	94 ± 3 (15%)	not detected
4b	0.1	92 ± 3 (11%)	not detected

Significant difference in electrophilicity between *o*-QMs **1** and **2** becomes evident when these species are generated in aqueous acetate buffer. Photolysis of **3b** in aqueous 0.1 M acetate buffer (pH 4.57 ± 0.05) produced the same products as in biphosphate buffer solutions, i.e., diol **3a** and *p*-quinone **5**. The product ratio, however, is reversed and **5** is a major product (Table 3). No detectable amounts of new products were observed. Irradiation of ether **4b** under the same conditions, on the other hand, produced substantial yield of 2-(acetoxymethyl)-4-methoxyphenol (**4d**, Scheme 3, Table 3). The latter is apparently formed by the attack of acetate ion on the electron-deficient methide carbon atom. Similar reactivity was also observed in the case of the parent *o*-QM.[17]

(15) (a) Itoh, T. *Prog. Polym. Sci.* **2001**, *26*, 1019. (b) Dolenc, J.; Sket, B.; Strlic, M. *Tetrahedron Lett.* **2002**, *43*, 5669.

(16) Modica, E.; Zanaletti, R.; Freccero, M.; Mella, M. *J. Org. Chem.* **2001**, *66*, 41.

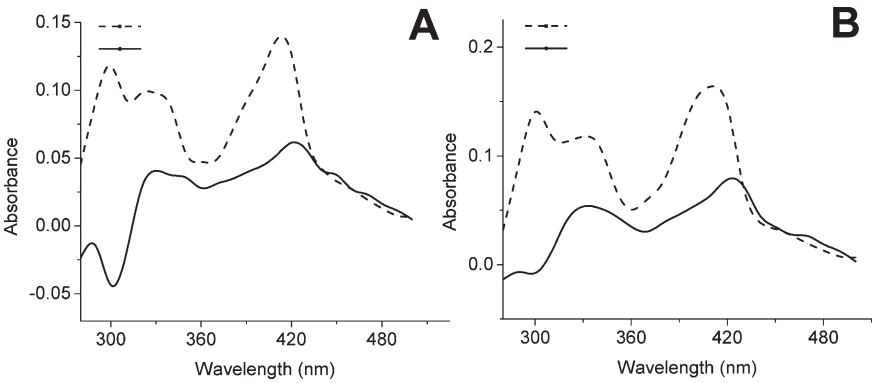

FIGURE 3. Transient spectra obtained at 5 μs (dashed line) and 1 ms (solid line) after the laser pulse in photolysis of ca. 0.1 mM aqueous solutions of **3a** (A) and **4a** (B) at pH 7.0.

TABLE 3. Photolysis of *o*-QM Precursors 3b and 4b in Aqueous Acetate Ion Buffer Solutions (0.1M buffer, pH 4.57± 0.05)

QM precursor	yield of **3a** or **4a**/% (conversion)[a]	yield of **4d**/% (conversion)[a]	yield of **5**/% (conversion)[a]
3b	27 ± 2 (29%)	no acetylation product	70 ± 2 (29%)
4b	66 ± 2 (13%)	31 ± 2 (13%)	not detected

[a] λ_{irr} = 300 nm; ca. 3 × 10^{-4} M in water.

Quinone methides are known to undergo very efficient hetero-Diels–Alder reactions with electron-rich alkenes.[4] Irradiation of **3a** and **4a** in aqueous acetonitrile in the presence of 30 mM ethyl vinyl ether resulted in the formation of adducts **6** and **7** in 90% isolated yields (Scheme 4).[12]

SCHEME 4

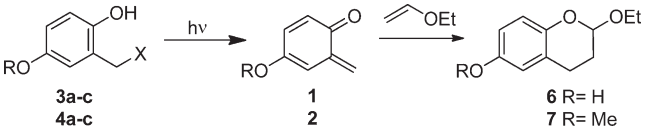

HPLC analysis shows near-quantitative formation of vinyl ether adducts in photolysis of alternative *o*-QM precursors **3b**,**c** and **4b**,**c** at both high and low conversions (Table 1). Products of *o*-QM hydration (**3a** and **4a**) or ketonization (**5**) were not detected in these experiments. The exclusive formation of Diels–Alder adduct despite the presence of more than a thousand-fold excess (33 M versus 0.03 M) of a nucleophilic solvent indicates that addition of ethyl vinyl ether to *o*-QMs is more than 2 orders of magnitude faster than a hydration reaction. Direct kinetic measurements of the rate of *o*-QM **1** and **2** reaction with ethyl vinyl ether were precluded by strong absorbance of 266 nm laser pulse by the alkene under experimental conditions ([QM precursor] = 10^{-4} M; [vinyl ether] = 0.02–0.1M).

Kinetics of the Formation and Reactions of 4-Hydroxy-6-methylene-2,4-cyclohexadien-1-one (1) and 4-Methoxy-6-methylene-2,4-cyclohexadien-1-one (2). Rate measurements were conducted in aqueous solutions at 25 ± 0.1 °C and ca. 10^{-4} M concentration of a substrate. Excitation of diols **3a** and **4a** with 4 ns 266 nm pulses of a Nd:YAG laser under these conditions results in the formation of short-lived transients ($\tau \approx 20\,\mu$s) with $\lambda_{max} \approx 410$ nm, which rapidly decay to yield new intermediates with $\lambda_{max} \approx 420$ nm (Figure 3). The latter transients, which were subsequently identified as *o*-QMs **1** and **2** (vide infra), decay at a relatively slower rate (τ = 3–8 ms). Since the formation and the decay of *o*-QMs proceed at very different rates, these processes were recorded in separate experiments with use of different time scales and signal amplifications. The experimental data were fitted separately for each transient to a double exponential function (Figure 4) and the first order rate constants were determined from the corresponding decay curve.[12]

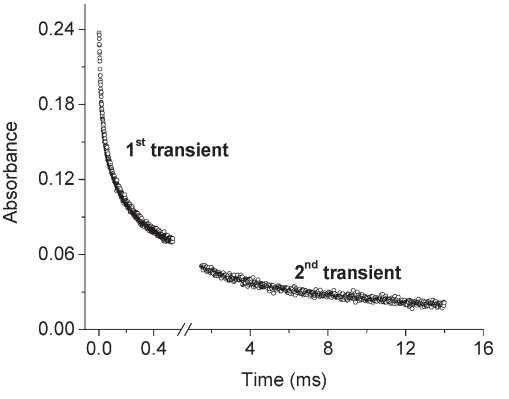

FIGURE 4. Formation and decay of *o*-QM **1** in the flash photolysis of ca. 0.1 mM aqueous solution of **3a** at pH 7.0.

The identity of the longer lived transients was established on the basis of their reactivity toward nucleophiles. Thus, decay of the second transients in wholly aqueous solution is relatively slow: k_{obs}(**3a**) = 300 ± 5 s^{-1} at pH 7.0; and k_{obs}(**4a**) = 126 ± 4 s^{-1} at pH 7.0. Addition of the azide ion dramatically increases the rate of this process: k_{N3}(**3a**) = 3.30 × 10^4 M^{-1} s^{-1}; and k_{N3}(**4a**) = 3.15 × 10^4 M^{-1} s^{-1} (Figure 5). On the other hand, the lifetime of the first transients generated from **3a** and **4a** was not affected by the presence of azide anion. Azide anion was previously demonstrated to increase the decay rate of *o*-QMs due to their pronounced electrophilicity.[11,18] Additional support for the structural assignments of the second transients came from the results of the laser flash photolyses of 2,5-dihydroxybenzyltrimethylammonium iodide **3c** and 2-hydroxy-5-methoxybenzyltrimethylammonium iodide **4c**. Photochemical decomposition of **3c** and **4c** produces the same set of products as the

(17) Chiang, Y.; Kresge, A. J.; Zhu, Y. *J. Am. Chem. Soc.* **2001**, *123*, 8089.

(18) Richard, J. P.; Amyes, T. L.; Bei, L.; Stubblefield, V. *J. Am. Chem. Soc.* **1990**, *112*, 9513.

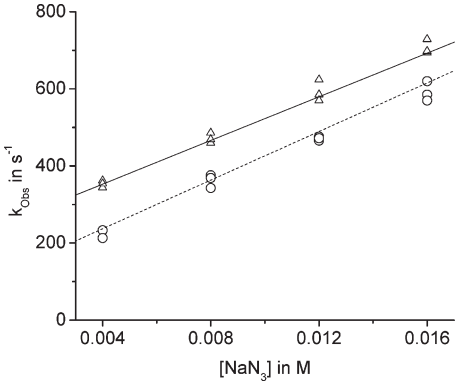

FIGURE 5. Quenching of *o*-QM **1** triangles) and **2** (circles) by sodium azide in aqueous solutions at pH 7.0.

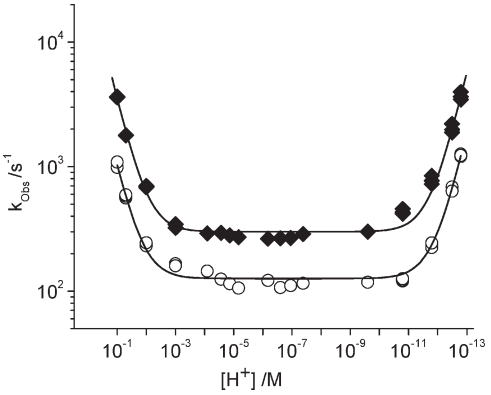

FIGURE 6. Rate profile for the hydration of *o*-QM **1** (solid squares) and **2** (open circles) in aqueous solution at 25 °C.

photolyses of **3a**,**b** and **4a**,**b**, which are produced from *o*-QMs **1** and **2**. However, only a single transient is observed in laser flash photolysis of ammonium salts **3c** or **4c**. The spectral properties, lifetime, and reactivity of these intermediates are identical, within the uncertainty limits, to that of the second transient generated from **3a** and **4a**.

Kinetics of Decay of *o*-QMs 1 and 2 in Aqueous Perchloric Acid, Sodium Hydroxide, and Buffer Solutions. Rates of the decay of *o*-QM **1** and **2** were determined in dilute aqueous solutions of perchloric acid and sodium hydroxide, as well as biphosphate ion, bicarbonate ion, and acetic acid buffers. The ionic strength of these solutions was kept constant at 0.1 M by adding sodium perchlorate as required. The rates of decay of the first transient observed in photolyses of **3a** and **4a** remain constant through the entire pH range. The decay of second transients, *o*-QMs **1** and **2**, on the other hand, is catalyzed by by perchloric acid, hydroxide ion, as well as some buffers (vide infra). Kinetic measurements in buffered solutions were performed in a series of solutions of varying buffer concentration but constant buffer ratio. The observed rates were then extrapolated to a zero buffer concentration. Relatively strong buffer catalysis was observed for the decay of both *o*-QMs **1** and **2** in acetate buffer solutions. However, only the rate of decay of *o*-QM **1** shows appreciable buffer catalysis in phosphate and bicarbonate buffer solutions. While the buffer catalysis for the decay of QM **2** in phosphate and bicarbonate buffer solution was very weak, the zero-concentration intercepts for the rate of decay of QM **2** were well-determined. The buffer-independent rate constants, together with observed rate constants determined in perchloric acid and sodium hydroxide solutions, are shown as the rate profile in Figure 6.

The rate of hydration of *o*-QMs **1** and **2** is independent of the acidity of aqueous solutions in the range from pH 4 to 10 resulting in a broad horizontal region in the rate profile (Figure 6). The observed rate constants on the plateau are $k_{H_2O} = 300 \pm 27\ s^{-1}$ for *o*-QM **1** and $k_{H_2O} = 126 \pm 16\ s^{-1}$ for *o*-QM **2**. The lower uncatalyzed hydration rate of *o*-QM **2** in comparison with the parent *o*-QM ($k_{H_2O} = 260\ s^{-1}$)[17] is apparently due to its reduced electrophilicty. In the case of *o*-QM **1** the lower rate of hydration is apparently augmented by the ketonization reaction. The decay rates of *o*-QMs **1** and **2** rise in a linear proportion to acid concentration: $k_{H^+}(\mathbf{1}) = (8.37 \pm 0.16) \times 10^3\ M^{-1}\ s^{-1}$; $k_{H^+}(\mathbf{2}) = (3.30 \pm 0.01) \times 10^4\ M^{-1}\ s^{-1}$ (Figure 7). The acid catalysis of the decay of the only

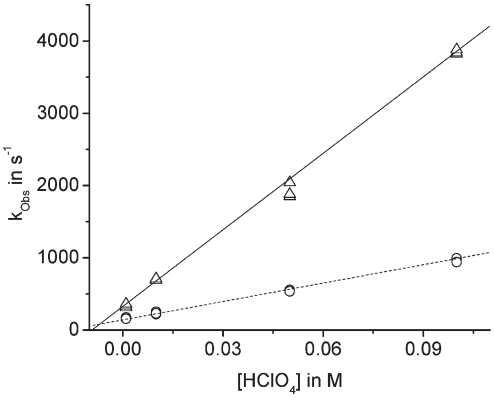

FIGURE 7. Specific acid catalysis observed of *o*-QMs **1** (triangles) and **2** (circles) generated from **3c** and **4** in aqueous perchloric acid.

transient observed in the photolyses of ammonium salts **3c** ($k_{H^+} = (8.12 \pm 0.10) \times 10^3\ M^{-1}\ s^{-1}$) and **4c** ($k_{H^+} = (3.49 \pm 0.07) \times 10^4\ M^{-1}\ s^{-1}$) is very similar to that of *o*-QMs generated from the diols **3a** and **4a**. This further confirms that the second transients observed in laser flash photolysis of **3a** and **4a** are indeed the *o*-QMs **1** and **2**, respectively. As in the case of the parent *o*-QM,[4b,19] the observed specific acid catalysis can be attributed to the rapid equilibration between *o*-QMs and more electrophilic *o*-hydroxybenzyl cations $\mathbf{1}^+$ and $\mathbf{2}^+$ (Scheme 5). The specific acid catalysis of the *o*-QM **2** hydration is somewhat weaker than that observed for the parent benzene-1,2-quinone methide ($k_{H^+} = 8.4 \times 10^5\ M^{-1}\ s^{-1}$),[4b,17] apparently due to the presence of the electron-rich methoxy group. Similar reduction of the electrophilicity of methide carbon by *m*-methoxy substitution was observed on addition of various nucleophiles to *o*-QMs.[5d] Electron-donating abilities of hydroxy and methoxy groups are close but acid catalysis of *o*-QM **1** decay is stronger than that of **2**. The higher acid sensitivity of **1** indicates that both hydration and ketonization reactions of this *o*-QM are catalyzed by acid. In fact, the **5** to **3a** ratio increases at higher hydronium ion concentration apparently due to stronger acid catalysis of the ketonization reaction (Table 2).

The decay of *o*-QMs **1** and **2** is also strongly catalyzed by the hydroxide ion: $k_{OH}(\mathbf{1}) = (3.51 \pm 0.19) \times 10^4\ M^{-1}\ s^{-1}$ and

(19) Keeffe, J. R.; Kresge, A. J. In *The Chemistry of Enols*; Rappoport, Z., Ed.; Wiley: New York, 1990; Chapter 7.

SCHEME 5

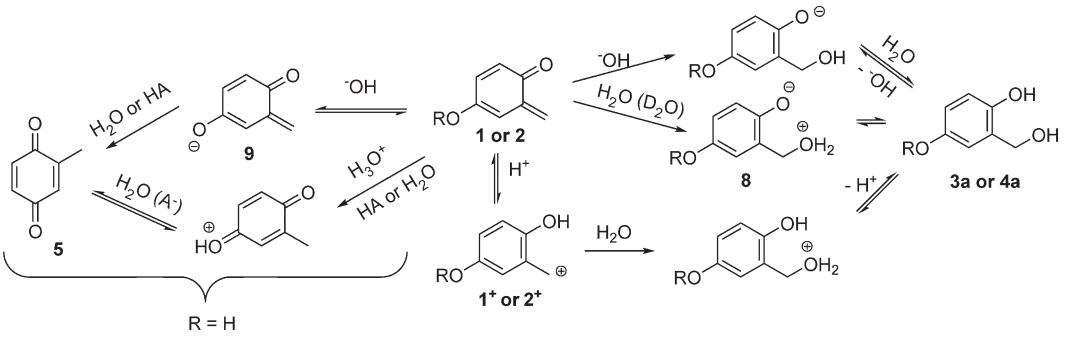

$k_{OH}(\mathbf{2}) = (1.08 \pm 0.02) \times 10^4\ M^{-1}\ s^{-1}$. The reactivities of *o*-QMs **1** and **2** toward nucleophilic attack by the hydroxide ion are very similar to those of the parent *o*-QM. However, the rate of hydration of **2** in aqueous sodium hydroxide solution is somewhat reduced in comparison to that of parent quinone methide ($k_{OH} = (3.0 \times 10^4\ M^{-1}\ s^{-1})$.[17] This is again attributed to the reduced electrophilicity of this *o*-QM due to electron-donating substituents in the ring.[5d] On the other hand, the hydroxide ion catalysis of the decay of **1** is more than three times stronger than that of **2**. This higher reactivity is due to the fact that the second pathway open to *o*-QM **1**, i.e., ketonization to **5**, is also catalyzed by a specific base.

The rate profiles of Figure 6 are readily understood in terms of the reaction Scheme 5. Thus, the major reaction consuming *o*-QM **2** in aqueous solutions is hydration to **4a**. *o*-QM **1**, on the other hand, reacts via two pathways: hydration to form **3a** and ketonization to *p*-quinone **5** (Scheme 5). The hydration mechanism of both *o*-QM **1** and **2** is very similar to that of the parent *o*-QM.[4b] In the base-catalyzed region of the rate profiles hydration apparently occurs via the rate-limiting attack of the hydroxide ion on the methide carbon of *o*-QMs **1** and **2**. Specific acid catalysis at pH < 3 should be assigned to the rapid pre-equilibrium protonation of the *o*-QM, which produces the more reactive cation $\mathbf{1}^+/\mathbf{2}^+$ (Scheme 5). The uncatalyzed portion of the rate profile at pH between 4 and 10 has two possible interpretations. The first is reversible protonation of the *o*-QMs by water, followed by rate-determining cation capture by the hydroxide ion so formed. As in the case of parent *o*-QM, this mechanism can be ruled out on the basis of the fact that it would require an impossibly large value of the rate constant for its rate-determining step.[19] The more probable mechanism of the pH-independent hydration is simple nucleophilic attack of water on the *o*-QM methylene group, with or without simultaneous proton transfer to avoid a zwitterionic intermediate **8** (Scheme 5).

Hydration of *o*-QM **1** to diol **3a** is accompanied by the tautomerization to methyl-*p*-quinone (**5**), which also shows acid and base catalysis. Conversion of *o*-QM **1** to **5** is, in fact, a vinylogous ketonization reaction. Such a process usually proceeds via rate-limiting proton transfer on a δ-carbon of a conjugated enol and, therefore, is catalyzed by general and specific acids.[19] Within the pH-independent part of the rate profile water takes over as the major protonating species. At pH > 9, the fraction of *o*-QM **1** existing in more reactive enolate form **9** grows with increasing pH producing an apparent hydroxide ion catalysis (Scheme 5).

Solvent isotope effects on the rate of *o*-QMs **1** and **2** consumption provide additional support for the mechanism in Scheme 5. Rate measurements were conducted in D_2O solutions of DCl in the range of concentrations from 0.001 to 0.1 M. The kinetic solvent isotopic effect on the acid-catalyzed hydration of **2** ($k_{H^+}/k_{D^+} = 0.48$) is very similar to that of the parent *o*-QM ($k_{H^+}/k_{D^+} = 0.42$).[5b] Such an inverse solvent isotopic effect is attributed to the rapid pre-equilibrium substrate protonation and is due to the fact that acids are weaker in D_2O and the fraction of more reactive protonated species $\mathbf{2}^+$ grows faster with D^+ concentration than with H^+.[20] The hydration reaction of **2** on the plateau region was slower in D_2O ($k_{H_2O}/k_{D_2O} = 1.63$). The nature of this isotope effect stems from the fact that positively charged O−H bonds, such as those in the intermediate **8** (Scheme 5), are looser than uncharged O−H bonds, such as those in a water molecule. Conversion of H_2O into ROH_2^+ leads to a loosening of the hydrogenic environment of the species involved, and that produces an isotope effect in the normal direction. Since the major reaction of the *o*-QM **1** within the pH 3−10 range is addition of water to produce **3a**, the observed solvent isotope effect ($k_{H_2O}/k_{D_2O} = 1.49$) is similar to that of **2**. In a sharp contrast with **2**, the isotope effect on acid-catalyzed (pH < 3) reactions of **1** is in the normal direction ($k_{H^+}/k_{D^+} = 1.60$). This observation can be explained by the fact that ketonization to methyl-*p*-quinone (**5**) becomes an increasingly important pathway of the *o*-QM **1** decay at higher acidities. The ketonization reaction, which is known to proceed via rate-determining proton transfer, is expected to produce a normal kinetic isotope effect (Scheme 5).[20,21]

Buffer Catalysis. The rate of *o*-QM **2** hydration shows virtually no dependence on the concentration of phosphate and bicarbonate buffer, resembling the behavior of the parent *o*-QM.[17] This observation agrees well with the nucleophilic hydration mechanism (Scheme 5). However, in the acetate buffer solutions, the rate of decay of *o*-QM **2** shows significant buffer catalysis. Rate measurements were performed in four series of solutions of varying acetate buffer concentrations but constant buffer ratio in each series. Slopes of buffer dilution plots at various buffer ratios represent pH-independent catalysis by the buffer components. As is evident from Figure 8, the efficiency of acetate

(20) Kresge, A. J.; More O'Ferrall, R. A.; Powell, M. F. In *Isotopes in Organic Chemistry*; Buncel, E., Lee, C. C., Eds.; Elsevier: New York, 1987; Chapter 4.

(21) (a) Capon, B.; Siddhanta, A. K.; Zucco, C. *J. Org. Chem.* **1985**, *50*, 3580. (b) Chiang, Y.; Guo, H.-X.; Kresge, A. J.; Tee, O. S. *J. Am. Chem. Soc.* **1996**, *118*, 3386. (c) Chiang, Y.; Kresge, A. J.; Santaballa, J. A.; Wirz, J. *J. Am. Chem. Soc.* **1988**, *110*, 5506. (d) Pruszynski, P.; Chiang, Y.; Kresge, A. J.; Schepp, N. P.; Walsh, P. A. *J. Phys. Chem.* **1986**, *90*, 3760. (e) Chiang, Y.; Kresge, A. J.; Nikolaev, V. A.; Popik, V. V *J. Am. Chem. Soc.* **1997**, *190*, 11183. (f) Capponi, M.; Gut, I. G.; Hellrung, B.; Persy, G.; Wirz, J. *Can. J. Chem.* **1999**, *77*, 605.

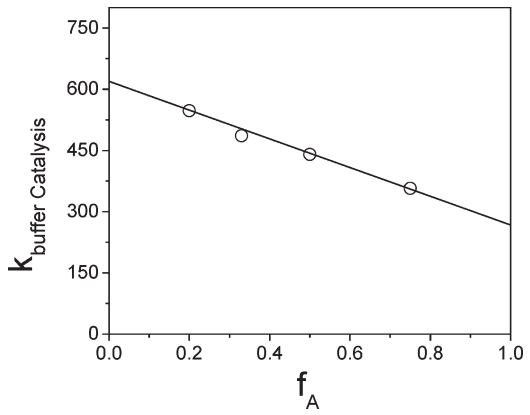

FIGURE 8. Dependence of the acetate buffer catalysis of *o*-QM **2** decay on the fraction of free acid in the buffer.

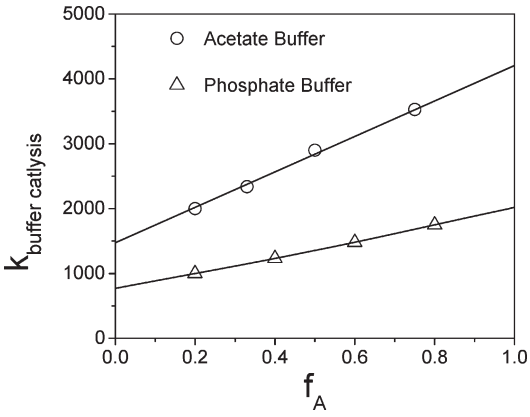

FIGURE 9. Dependence of the buffer catalysis of the decay of *o*-QM **1** on the fraction of free acid in the buffer.

buffer catalysis decreases with increased fraction of free acid. This observation, as well as the observed formation of acetylation product **4d** (Scheme 3, Table 3), indicate the nucleophilic nature of the acetate buffer catalysis of *o*-QM **2** hydration. Similar reactivity was also observed in the case of the parent *o*-QM.[17]

In a contrast to *o*-QM **2**, the rate decay of *o*-QM **1** is more sensitive to the free acid concentration in both phosphate and acetate buffer solutions (Figure 9). The strong buffer catalysis of the decay of *o*-QM **1** observed in all buffers examined can be explained by the fact that the ketonization reactions are usually catalyzed by general acid (Scheme 5).[22] Thus, in 0.1 M acetate buffer *o*-QM **1** does not form any detectable amounts of new products, but the ratio of ketonization to hydration products increases dramatically (Table 3). Buffer catalytic coefficients can be partitioned into contributions from the acidic and basic components by extrapolation of the plots in Figure 9 to $f_A = 1$ (general acid: $k_{H_2PO_4^-} = (1.99 \pm 0.02) \times 10^3\ M^{-1}\ s^{-1}$; $k_{HOAc} = (4.20 \pm 0.11) \times 10^3\ M^{-1}\ s^{-1}$) and $f_A = 0$ (general base catalysis: $k_{HPO_4^{2-}} = (7.40 \pm 0.02) \times 10^2\ M^{-1}\ s^{-1}$; $k_{AcO^-} = (1.44 \pm 0.05) \times 10^3\ M^{-1}\ s^{-1}$). Ketonization reaction in buffer solutions can also occur by ionization of *o*-QM **2** to the enolate ion **9** followed by the proton transfer from the buffer acid (Scheme 5). The first step of this mechanism will produce hydroxide ion catalysis and the second is catalyzed by a general acid. Combination of these to catalyses is operationally equivalent to a general base catalysis.

Elucidation of the *o*-QMs Precursor Structures. In agreement with previous reports,[4b] parent *o*-QM is formed within the duration of a laser pulse in the flash photolysis of *o*-hydroxybenzyl alcohol. We observed similar "instant" formation of *o*-QMs **1** and **2** in photolyses of ammonium precursors **3c** and **4c**. In a sharp contrast with these results, laser flash photolysis of 2-(hydroxymethyl)benzene-1,4-diol (**3a**) and 2-(hydroxymethyl)-4-methoxyphenol (**4a**), as well as their ether analogues **3b** and **4b**, allowed us to detect a short-lived ($\tau \approx 20\ \mu s$) kinetic precursor to *o*-QMs. In unbuffered aqueous solutions *o*-QM **1** is produced with the observed rate $k = (4.80 \pm 0.20) \times 10^4\ s^{-1}$ and *o*-QM **2** with $k_{obs} = (5.00 \pm 0.45) \times 10^4\ s^{-1}$. The rate of *o*-QMs formation is independent of pH of the solution and is not affected by the presence of the azide ion. The fluorescence lifetimes of **3a** and **4a** ($\tau \approx 8$ ns) are much shorter than the rise time of the corresponding *o*-QMs, indicating that the latter species are not formed directly from the singlet excited state of the diol precursors. Saturation of the solution with oxygen or addition of increased amounts 1,3-cyclohexadiene to the reaction mixture before the photolysis do not quench the first transient or affect the rate of its decay. This observation allows us to conclude that triple excited states of **3a** and **4a** are not involved in the formation of the respective *o*-QMs. The zwitterionic structure **8**, which can be potentially formed in ESIPT to benzylic oxygen atom in **3a** or **4a** (Scheme 6), is an unlikely candidate for *o*-QM precursor because reverse proton transfer in this structure should proceed at least at the diffusion-controlled rate limit. In fact, pH insensitivity of the first transient allows us to exclude all ionized forms of **3a** and **4a** from consideration.

SCHEME 6

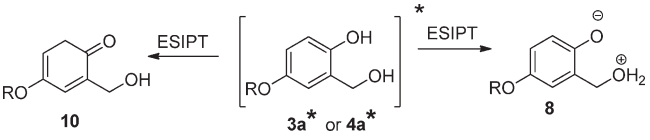

ESIPT from the phenolic oxygen to the aromatic carbon is well documented for phenols and naphthols.[22] Such carbon protonation leading to the unstable keto-form of phenol (such as **10**, Scheme 5, or its isomers) should result in incorporation of deuterium in hydration products when photolysis is conducted in deutrated solvents. GC-MS analysis of the products formed after prolonged irradiation of diols **3a** and **4a** in D_2O showed no deuterium enrichment in the aromatic rings. This observation allows us to rule out participation of **10** or isomeric structures. It has been shown, on the other hand, that *o*-quinone methides might reversibly isomerize to benzoxete derivatives, which are stable only at cryogenic temperatures.[23] A similar ring-opening reaction is actually used for the generation of thio-*o*-quinone methides from benzothietes.[24] We have recently reported

(22) (a) Lukeman, M.; Wan, P. *J. Am. Chem. Soc.* **2003**, *125*, 1164. (b) Lukeman, M.; Veale, D.; Wan, P.; Munasinghe, V. R. N.; Corrie, J. E. T. *Can. J. Chem.* **2004**, *82*, 240. (c) Basaric, N.; Wan, P. *J. Org. Chem.* **2006**, *71*, 2677.

(23) (a) Qiao, G. G.; Lenghaus, K.; Solomon, D. H.; Reisinger, A.; Bytheway, I.; Wentrup, C. *J. Org. Chem.* **1998**, *63*, 9806. (b) Tomioka, H. *Pure Appl. Chem.* **1997**, *69*, 837. (c) Sauter, M.; Adam, W. *Acc. Chem. Res.* **1995**, *28*, 289. (d) Shanks, D.; Frisell, H.; Ottosson, H.; Engman, L. *Org. Biomol. Chem.* **2006**, *4*, 846.

(24) (a) Mayer, A.; Meier, H. *Tetrahedron Lett.* **1994**, *35*, 2161. (b) Meier, H.; Mayer, A.; Groschl, D. *Sulfur Rep.* **1994**, *16*, 23 and references cited therein. (c) Meier, H.; Eckes, H.-L.; Niedermann, H.-P.; Kolshorn, H. *Angew. Chem., Int. Ed. Engl.* **1987**, *26*, 1046. (d) Kanakarajan, K.; Meier, H. *J. Org. Chem.* **1983**, *48*, 881.

SCHEME 7

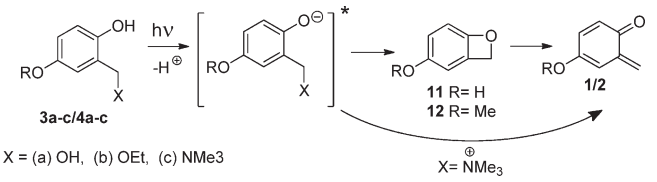

the detection of naphthoxete precursors of naphthoquinone methides.[11] We, therefore, believe that oxetanes **11** and **12** are the likely precursors of *o*-QMs **1** and **2** (Scheme 7).

Since the fluorescence spectra of **3a** and **4a** are very similar to spectra of corresponding phenols,[25] we can assume that excitation of these substrates results in the formation of the phenolate ions in the excited state. If the *o*-benzylic position is substituted with a good leaving group (e.g., X = NMe_3^+, Scheme 7), the *o*-QM is formed directly from the phenolate ion. However, in case of poor leaving groups (e.g., X = OH or OR), oxetane is formed. The latter then opens up in a ground state reaction to give an *o*-QM. Ring-opening of **11** and **12** to give *o*-QMs **1** and **2** is an electrocyclic reaction and, therefore, is not sensitive to acid/base catalysis or the presence of reactive nucleophiles such as azide ion.

Conclusions

Two *o*-quinone methides, 4-hydroxy-6-methylene-2,4-cyclohexadien-1-one (**1**) and 4-methoxy-6-methylene-2,4-cyclohexadien-1-one (**2**), are efficiently generated by the irradiation of three different types of precursors: substituted *o*-hydroxybenzyl alcohols **3a** and **4a**; their ethyl ethers **3b** and **4b**, as well as (2,5-dihydroxy-1-phenyl)methyl- (**3c**) and (2-hydroxy-5-methoxy-1-phenyl)methyltrimethylammonium iodides (**4c**). The reactivity of *o*-QMs **2** resembles that of other *o*-quinone methides albeit with reduced nucleophilicity. In aqueous solution it undergoes efficient rehydration back to **4a** and this reaction is catalyzed by both hydroxide and hydronium ions. In the case of *o*-QMs **1**, addition of water to give **3a** competes with tautomerization to form methyl-*p*-quinone (**5**). This is a rather unique phenomenon, as the same carbon atom shows both electrophilic (addition of water) and nucleophilic (protonation) reactivity. The ketonization reaction shows pronounced general acid catalysis. Both *o*-QMs readily react with other nucleophiles such as azide anion and undergo efficient Diels−Alder cycloaddition to electron-rich olefins. Photochemical dehydration of **3a** and **4a** to produce *o*-QMs **1** and **2** proceeds via the formation of a reactive intermediate. On the basis of the reactivity of these transient species the benzoxete structures **11** and **12** were assigned to these transients.

Experimental Section

General Methods. All organic solvents were dried and freshly distilled before use. Flash chromatography was performed with 40−63 μm silica gel. All NMR spectra were recorded in $CDCl_3$ and referenced to TMS unless otherwise noted. Solutions were prepared with HPLC grade water, methanol, and acetonitrile. Substrate concentration for kinetics experiments was kept at ca. 1×10^{-4} M for **3a** and **4a** and 5×10^{-5} M for **3c** and **4c**. Solutions of ca. 3×10^{-4} M of compounds **3b**, **3c**, **4b**, and **4c** were irradiated in water and in the presence of ethyl vinyl ether (3×10^{-2} M) in 50% MeCN in water, using a mini-Rayonet photochemical reactor equipped with eight fluorescent UV lamps (4 W, 300 nm). Reaction mixtures after photolysis were analyzed by HPLC and chemical yields were determined from the calibration plot constructed with known standards of the pure product. Quantum efficiencies of photochemical reactions were measured by ferrioxalate actinometry.[26] Buffer solutions for kinetic experiments were prepared by using literature pK_a values of the buffer acids and activity coefficient recommended by Bates.[27]

Kinetic Experiments. Rate measurements were conducted with a nanosecond kinetic spectrometer equipped with a Nd:YAG laser (pulse width = 4 ns) fitted with second and fourth harmonic generators. Degassed solutions of *o*-QM precursors with OD $\approx$ 0.4 were thermostated at 25 $\pm$ 0.05 °C. Since the formation and the decay of *o*-QMs proceed at very different rates, these processes were recorded in separate experiments with different time scales and signal amplifications. The experimental data were fitted separately for each transient to a double exponential function and the first order rate constants were determined from the corresponding decay curve. Second order rate constant of *o*-QM reactions with azide ion were determined from the plot of the concentration of the trapping reagents vs the observed pseudo-first-order rate constants. The experimental rate constants are summarized in Tables S1−S20 in the Supporting Information.[12]

Fluorescent Measurements. Fluorescent spectra of **3a** and **4a** were recorded at λ_{ex} = 305 nm in doubly deionized water with the substrate concentration ca. 1×10^{-5} M, using Varian steady state fluorimeter. The excitation source slits and the detector slits were set to 2 and 5 nm, respectively. The fluorescence quantum yields were determined with phenol as the standard reference.[27,28]

Materials. Ethyl vinyl ether and sodium were purchased from Sigma-Aldrich and used as received. 2-(Hydroxymethyl)benzene-1,4-diol (**3a**),[29] (2-(hydroxymethyl)-4-methoxyphenol (**4a**),[30] (2-hydroxy-5-methoxy-1-phenyl)methyltrimethylammonium iodide (**4c**),[5d] and 2-(acetoxymethyl)-4-methoxyphenol (**4d**)[31] were prepared following the literature procedures.

2-(Ethoxymethyl)benzene-1,4-diol (3b). A solution of **3a** (70 mg, 1 mmol) in 80% aqueous ethanol (500 mL) was irradiated, using a mini-Rayonet photochemical reactor equipped with 254 nm lamps for 1 h. Photolysate was extracted with ethyl acetate then dried over sodium sulfate; solvents were removed under vacuum. The residue was separated by chromatography (30% EtOAc in hexane) to give 50 mg (60%) of **3b** as a colorless oil. ^{1}H NMR δ 6.72−6.74 (m, 1H), 6.65−6.67 (m, 1H), 6.52−6.53 (m, 1H), 4.61 (s, 2H), 3.60 (q, 2H, J = 5.2 Hz), 1.26 (t, 3H, 5.2 Hz). ^{13}C NMR δ 149.8, 148.9, 123.4, 117.3, 116.1, 115.1, 71.9, 66.5, 15.2; GC-MS m/z (%) 168 (10), 138 (100), 137 (40), 122 (60), 121 (25), 110 (65), 94 (50), 82 (37), 63 (45), 53 (47). FW calcd for $C_9H_{12}O_3^+$ 168.0786; EI-HRMS found 168.0783.

2-(Ethoxymethyl)-4-methoxyphenol (4b). Concentrated HCl (5 mL) was added to a solution of **4a** (500 mg, 3.25 mmol) in 95% aqueous ethanol (20 mL), then the reaction mixture was stirred

(25) (a) Wehry, E. L.; Rogers, L. B. *J. Am. Chem. Soc.* **1965**, *87*, 4234. (b) Stalin, T.; Devi, R. A.; Rajendiran, N. *Spectrochim. Acta* **2005**, *61A*, 2495.

(26) Murov, S. L.; Carmichael, I.; Hug, G. L. In *Handbook of Photochemistry*; Marcel Dekker: New York, 1993; p 299.

(27) Bates, R. G. *Determination of pH Theory and Practice*; Wiley: New York, 1973; p 49.

(28) Berlman, I. B. *Handbook of Fluorescence Spectra of Aromatic Molecules*; Academic Press: New York, 1971; p 473.

(29) Casiraghi, G.; Casnati, G.; Puglia, G.; Sartori, G. *Synthesis* **1980**, *2*, 124.

(30) Ono, M.; Kawashima, H.; Nonaka, A.; Kawai, T.; Haratake, M.; Mori, H.; Kung, M. P.; Kung, H. F.; Saji, H.; Nakayama, M. *J. Med. Chem.* **2006**, *49*, 2725.

(31) Bray, C. D. *Synlett* **2008**, *16*, 2500.

for 3 h at rt and poured onto crushed ice. The aqueous layer was extracted with ethyl acetate and dried over sodium sulfate; solvents were removed under vacuum. The crude product was purified by column chromatography (40% dichloromethane in hexane) to give **4b** as a yellow oil (366 mg, 62%). ^{1}H NMR δ 7.27 (br s, 1H), 6.72−6.80 (m, 2H), 6.56−6.57 (m, 1H), 4.64 (s, 2H), 3.72 (s, 3H), 3.58 (q, 2H, J = 5.2 Hz), 1.25 (t, 3H, 5.2 Hz). ^{13}C NMR δ 153.2, 150.3, 123.3, 117.3, 114.5, 113.9, 72.3, 66.5, 56.0, 15.3. GC-MS m/z (%) 182 (20), 136 (100), 137 (20), 108 (45), 79 (20), 65 (20). FW calcd for $C_{10}H_{14}O_3^+$ 182.0943; EI-HRMS found 182.0943.

(2,5-Dihydroxy-1-phenyl)methyltrimethylammonium Iodide (3c). A solution of 2,4-dihydroxybenzaldehyde (900 mg, 6.67 mmol) in methanol (15 mL) was added to a mixture of 1.16 g (14.2 mmol) of dimethylamine hydrochloride, sodium acetate (0.91 g, 11.1 mmol), and 0.49 g (7.7 mmol) of sodium cyanoborohydride in methanol (30 mL).The pH of the solution was maintained throughout the reaction in the range 7−8 by the addition of concentrated HCl. The solution was stirred at room temperature during 24 h. Acetone (50 mL) was added and the solution was acidified to pH 2−3 with 6 N HCl solution. Solvents were removed under vacuum, and the residue was redissolved in water (15 mL) and washed with ether (4 × 15 mL). NaOH solution was added to the remaining aqueous phase until pH reached 8−9. The resulting aqueous solution was extracted with ether (6 × 25 mL), the organic layer was dried over $MgSO_4$, and solvent was removed under vacuum. The fractional distillation of amber oil residue produced 0.8 g of pure 2-(*N*,*N*-dimethylaminomethyl)benzene-1,4-diol (71% yield) as a colorless oil. ^{1}H NMR (400 MHz, $CDCl_3$) δ 6.62−6.50 (m, 3H), 3.54 (s, 2H), 2.28 (s, 6H). ^{13}C NMR (100 MHz, $CDCl_3$) δ 151.1, 149.9, 123.0, 116.1, 115.4, 115.0, 62.6, 43.9. GC-MS m/z (%) 168 (10), 167 (45), 152 (6), 122 (12), 94 (15), 58 (25), 44 (100).

Methyl iodide (1.5 mL) was added to a stirred solution (0 °C) of 2-(*N*,*N*-dimethylaminomethyl)benzene-1,4-diol (450 mg, 2.5 mmol) in acetonitrile (1.5 mL) and the mixture was stirred for 2 h at rt. Anhydrous ether (25 mL) was added to the reaction mixture, and white precipitate separated and was washed with ether to give 0.8 g (98%) of quaternary ammonium salt **3c** as a white solid. ^{1}H NMR (400 MHz, D_2O) δ 6.78−6.86 (m, 3H), 4.29 (s, 2H), 3.63 (s, 3H), 2.99 (s, 9H). ^{13}C NMR (100 MHz, D_2O) δ 150.0, 148.7, 120.6, 119.7, 117.8, 115.4, 64.1, 52.7. GC-MS m/z (%) 182 (7), 181 (45), 168 (10), 168 (5), 167 (30), 149 (8), 137 (52), 136 (40), 123 (12), 108 (17), 94 (12), 73 (17), 70 (37), 61 (50), 53 (27), 44 (62), 45 (100). FW calcd for $C_{10}H_{16}NO_2^+$ 182.1181; EI-HRMS found 182.1188.

2-Ethoxy-6-hydroxychroman (6). A solution of **3a** (42 mg, 0.3 mmol) and ethyl vinyl ether (2.9 mL, 30 mmol) in aqueous acetonitrile (1:1, 300 mL) was irradiated, using a mini-Rayonet photochemical reactor equipped with 254 nm lamps for 1 h. Photolysate was extracted with ethyl acetate and dried over sodium sulfate; solvents were removed under vacuum. The residue was separated by chromatography (20% EtOAc in hexane) to give 53 mg (90%) of **6** as a colorless oil. ^{1}H NMR (400 MHz, $CDCl_3$) δ 6.69−6.70 (m, 1H), 6.53−6.60 (m, 2H), 5.20 (t, 1H, J = 2.8 Hz), 3.82−3.88 (m, 1H), 3.59−3−64 (m, 1H), 2.88−2.97 (m, 1H), 2.60, 2.55−2.59 (m, 1H), 1.88−2.03 (m, 2H), 1.18 (t, 3H, 7.6 Hz). ^{13}C NMR (100 MHz, $CDCl_3$) δ 149.3, 146.3, 123.71, 117.8, 115.6, 114.5, 96.9, 63.8, 26.7, 20.9, 15.3. GC MS m/z 195 (10), 194 (90), 149 (30), 148 (70), 147 (100), 122 (50), 94 (30), 77 (20), 65 (25), 55 (28), 45 (15). FW calcd for $C_{11}H_{14}O_3$ 194.0943, EI-HRMS found 194.0952.

2-Ethoxy-6-methoxychroman (7). Compound **7** was prepared in 91% yield following the same procedure that was described for **6**. The spectral properties are consistent with the previously reported values.[32] ^{1}H NMR (400 MHz, $CDCl_3$) δ 6.69−6.78(m, 2H), 6.61−6.62 (m, 1H), 5.23 (t, 1H, J = 2.8 Hz), 3.84−3.90 (m, 1H), 3.76 (s, 3H), 3.60−3−66 (m, 1H), 2.94−3.02 (m, 1H), 2.60−2.66 (m, 2H), 1.90−2.07 (m, 2H), 1.20 (t, 3H, J = 7.6 Hz). ^{13}C NMR of **2** (100 MHz, $CDCl_3$) δ 153.8, 146.3, 123.5, 117.7, 114.1, 113.5, 97.0, 63.8, 55.9, 26.8, 21.2, 15.4. GC MS m/z 208 (100), 180 (5), 163 (30), 162 (35), 161 (40), 147 (8), 136 (75), 108 (27), 91 (12), 73 (12), 65 (12), 55 (7), 43 (5). FW calcd for $C_{12}H_{16}O_3$ 208.1099, EI-HRMS found 208.1102.

Acknowledgment. The authors thank the National Science Foundation (CHE-0449478) and the donors of the ACS Petroleum Research Fund (434444-AC4) for the support of this project.

Supporting Information Available: Tables of raw kinetic measurements and NMR spectra of newly synthesized compounds. This material is available free of charge via the Internet at http://pubs.acs.org.

(32) Manetsch, R.; Zheng, L.; Reymond, M. T.; Woggon, W.-D.; Reymond, J.-L. *Chem.—Eur. J.* **2004**, *10*, 2487.